Density Functional Theory [B3LYP/6-311G(d,p)] Study of a New Copolymer Based on Carbazole and (3,4-Ethylenedioxythiophene) in Their Aromatic and Polaronic States

Z. El Malki,[1,2] S. M. Bouzzine,[2] L. Bejjit,[1] M. Haddad,[1] M. Hamidi,[2,3] M. Bouachrine[2,4]

[1]*Laboratoire LASMAR (URAC 11), Faculté des Sciences, Université Moulay Ismail Meknès, Maroc*
[2]*URMM/UCTA, FST Errachidia, Université Moulay Ismaïl, Meknès, Maroc*
[3]*Faculté Polydisciplinaire d'Errachidia, Université Moulay Ismaïl, Meknès, Maroc*
[4]*MIM, Faculté Polydisciplinaire de Taza, Université Sidi Mohamed Ben Abdellah, Taza, Maroc*

Received 23 November 2010; accepted 22 February 2011
DOI 10.1002/app.34395
Published online 12 July 2011 in Wiley Online Library (wileyonlinelibrary.com).

ABSTRACT: We report a theoretical study of a new copolymer based on (Carbazole and Ethylenedioxythiophene)$_n$ (n = 1–3) in their neutral and oxidized states, by using B3LYP/6-311G(d,p) calculations and thus deduce its optoelectronic properties. We discuss the influence of chain length of these properties. We also discuss the experimental UV-Visible spectrum for (Polyvinylcarbazole-Poly(3,4-ethylenedioxythiophene)) (PVK-PEDOT) copolymer powder for comparison. Conformational analysis shows that there are no big changes in the structural parameters of the oligomers in their neutral form. After oxidation the oligomers become more planar and show a quinoidal character. The electronic states of monomers (Cbz-Edot) based Carbazole (Cbz) and Ethylenedioxythiophene (Edot), were elucidated by molecular orbital calculations using B3LYP/6-311G(d,p). The HOMO, LUMO, and gap energies E_g were also deduced for the stable structure of the neutral, polaronic, and bipolaronic forms. Electronic transition energies and oscillator strengths of copolymers were obtained by the ZINDO, TD-DFT, and CIS methods. Band gaps of the corresponding polymers were obtained by extrapolating oligomer gaps to infinite chain lengths. These results will be compared with the experimental values obtained by optical spectrum. The optoelectronic properties of the (Cbz-Edot)$_3$ led us to suggest that this oligomer is a good model to reflect those of the parent polymer. © 2011 Wiley Periodicals, Inc. J Appl Polym Sci 122: 3351–3360, 2011

Key words: conjugated polymers; conformational analysis; molecular modeling; structure-property relations; oligomers

INTRODUCTION

Conjugated oligomers have been extensively studied and have attracted considerable attention as a novel class of semiconductors because of their interesting electronic properties.[1]

Most of recent papers are focused on the polyvinylcarbazole (PVK),[2–4] due to its important specific properties (photoconductivity, photoluminescence, and hole transport properties). The polymerization of *N*-Vinylcarbazole (NVK) as well as the structure and properties of NVK and PVK are largely controlled by the electronic and steric influence of the carbazole group. Although the electronegative nitrogen atom withdraws electrons from the double bond through an inductive effect, the mesmeric effect of nitrogen which donates its unshared electron pair, offsets the electron withdrawing effect and create an electron-rich conjugated system.[5] The ground states of the carbazole-based oligomers, were recently studied by Yang et al.,[6] using the DFT method and the low-lying excited states using the time dependent density functional theory, a satisfactory linear relationship was found between experimental data and the excitation energy obtained from TD-DFT calculations.

On the other hand, Poly(3,4-ethylenedioxythiophene) (PEDOT),[7,8] has excellent transparency in the visible region, good electrical conductivity, and environmental stability. As antistatic material, PEDOT has been recently exploited extensively for practical applications. The most interesting aspects related to the synthesis and the characterization of that polymer have been reviewed recently.[9] Doped Poly(3,4-ethylenedioxythiophene) (PEDOT) is one of the most successful conducting polymers. It combines a high conductivity in the oxidized state with good stability under ambient conditions.[10–13] In this polymer the oxygen atoms of the dioxane ring are directly

Correspondence to: Z. El Malki (zelmalki@yahoo.fr).

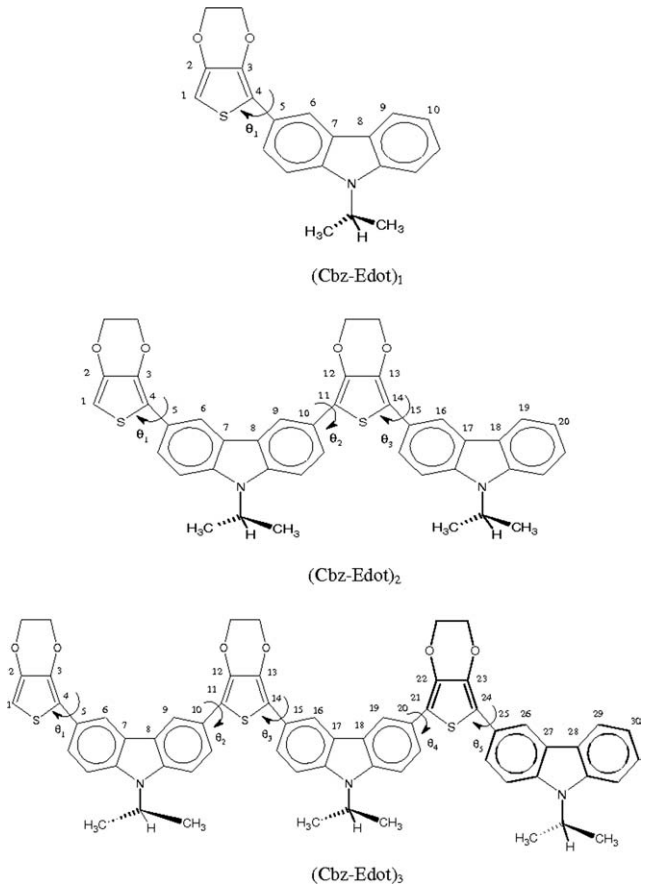

Figure 1 Structures of studied oligomers $(Cbz\text{-}Edot)_n$.

attached to the 3 and 4 positions, exerting an electron-donating effect that reduces the band gap of polythiophene. Quantum-chemical calculations have been recently employed to investigate different aspects related to the molecular and electronic structure of PEDOT.[14] Dkhissi et al.[15] investigated the relative stability of the aromatic and quinoid-like structures for neutral PEDOT using *ab initio* SCF and DFT calculations at the HF and B3LYP levels, respectively. Materials that combine properties of these two polymers (PVK and PEDOT)[16,17] are attractive materials for a variety of applications in the electronic devices, such as light-emitting diodes (LED) and field-effect transistors (FET).[18–22] Generally, the electric properties of polymers PVK and PEDOT are strongly governed by the intramolecular delocalization of π electrons along the conjugation chain. This delocalization depends on the extent of the overlapping between the p_z orbital of the carbon atoms in positions α and β of adjacent monomers and, therefore, is dominated by the rotation around the C_α-C_β bond.

In this contribution we wish to examine the structural and electronic properties of $(Cbz\text{-}Edot)_n$ (n = 1–3) oligomers, in their neutral and oxidized states, as obtained with the B3LYP/6-311G(d,p) calculations. The electronic transition energies and oscillator strengths results were obtained by ZINDO, TD-DFT, and CIS methods, and to compare these data to the corresponding properties of the experimental absorption results for (PVK-PEDOT) copolymer.

METHODOLOGIES AND COMPUTATION

We used in our calculation, the DFT method of three-parameter compound of Becke (B3LYP),[23] of the neutral, polaronic, and bipolaronic oligomers by $(Cbz\text{-}Edot)_n$, for n = 1–3. The 6-311G(d,p) basis set was used for all calculations.[24–27]

For the neutral state, the conformational analysis was done by changing the torsional angles θ between adjacent units (Cbz and Edot) by 20° steps in the same direction.

We shall determine the final torsional angle and the intercyclic distances of the conformation in each minimum. To obtain the structures optimized by polymers charged, we used the optimized structures by the neutral form. All oligomer structures obtained for polaronic and bipolaronic states become more planar.

The wavelengths, electronic transition energies and oscillator strengths of the various structures in their stable states are calculated by using various methods (semiempirical ZINDO,[28] configuration interaction singles (CIS)[29] and time dependent density functional theory (TD-DFT)[30]).

The HOMO, LUMO, and E_g (between HOMO and LUMO) were also calculated for the stable structure of the neutral, oxidized forms. We employed the linear extrapolation technique in this research, which has been successfully employed to investigate several series of polymers.[31,32] We compare the results determined by the calculation with the value deducted from the absorption curve.

The calculations, of the studied oligomers, have been performed by the Gaussian 03 program package.[33]

RESULTS AND DISCUSSION

In this work, we are interested in understanding the change in the structure and optoelectronic properties with the chain length, we would like to describe the actual extent of oxidized states (polaron and bipolaron) without interferences from chain-end effects and also to deal with conjugation lengths similar to those encountered in parent polymers.[16] Secondly, our aim is to find a model that reflects the polymer properties.

Neutral structure

We plot in Figure 1, the structures of the oligomers $(Cbz\text{-}Edot)_n$ (n = 1–3), with the bond lengths and the dihedral angles θ of the studied molecules.

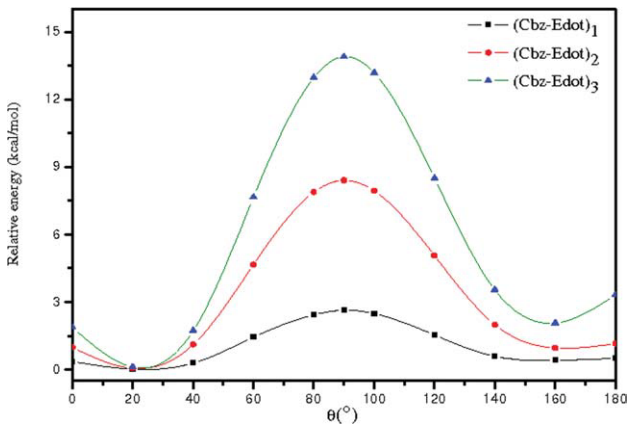

Figure 2 Potential energy curves of $(Cbz\text{-}Edot)_n$ (n = 1–3) obtained by B3LYP/6-311G(d,p) level. [Color figure can be viewed in the online issue, which is available at wileyonlinelibrary.com.]

Conformational analysis

The variation of the relative energy or the torsion potential (ΔE_{rel}) is the difference of energy between every conformation (E_{conf}) and the most stable conformation ($E_{conf.Stab}$): $\Delta E_{rel} = E_{conf} - E_{conf.Stab}$, according to the torsional angles θ_i. The potential energy of the several oligomers $(Cbz\text{-}Edot)_n$ (n = 1–3), obtained with B3LYP/6-311G(d,p) level, are shown in Figure 2. All the curves obtained for the oligomers $(Cbz\text{-}Edot)_n$ have the same behavior and they present five extrema, three maxima situated at 0, 90, and 180° and two minima located at about 20 and 160°. The potential energy curves show the existence, for all oligomers, of two stable conformations: a syngauche conformation and antigauche conformation with the syn-one being the most stable (Table I).

We list in Table II the relative energy of all conformations of the several oligomers $(Cbz\text{-}Edot)_n$ (n = 1–3), calculated by B3LYP/6-311G(d,p) level. The all conformations relative energies increase with the chain length while the syngauche relative energy remains identical for all oligomers. Furthermore, while at both computational level the difference between the syngauche and antigauche is about 0.086 eV for $(Cbz\text{-}Edot)_3$. This shows that the steric effect felt altered with the increase of rings number.

TABLE I
Angle of Torsion (°) Cisoide and Transoide Conformation of Copolymers $(Cbz\text{-}Edot)_n$ (n =1–3), Obtained by B3LYP/6-311G(d,p) Level, for the Neutral Form

Number of monomers	1	2	3
θ_1(syngauche)	25.2	23.9	26.2
θ_1(antigauche)	153.8	153.4	154.8
θ_2 (syngauche)	–	24.0	24.6
θ_2(antigauche)	–	170.5	155.4
θ_3(syngauche)	–	23.5	23.4
θ_3(antigauche)	–	157.5	156.2
θ_4(syngauche)	–	–	24.1
θ_4(antigauche)	–	–	164.3
θ_5(syngauche)	–	–	22.5
θ_5(antigauche)	–	–	161.6

TABLE II
Relative Energy (eV) of All Conformations of All Oligomers $(Cbz\text{-}Edot)_n$ (n =1–3) for the Neutral Form, Calculated by B3LYP/6-311G(d,p) Level

Oligomers	Syn (0°)	Syngauche	Perpendicular	Antigauche	Anti (180°)
1	0.016	0.000	0.115	0.017	0.022
2	0.043	0.000	0.365	0.039	0.051
3	0.081	0.000	0.603	0.086	0.144

Geometric properties

The optimized structure of the oligomer $(Cbz\text{-}Edot)_3$, for the neutral form, obtained with the B3LYP/6-311G(d,p) level, are shown in Figure 3. The bond lengths of molecules at their global minima, and the dihedral angles (θ_i, i = 1–5), for their neutral form, as computed at B3LYP/6-311G(d,p) level, are collected in Table III. There are no significant differences among the bond lengths obtained for all oligomers in their ground state.

The same observations are obtained for (Cbz-furane) with HF/6-31G(d) (planar conformation and inter-ring distance is about 1.467 Å),[34] but when we substituted Furane by Edot or thiophene we note that the dihedral angle and the inter-ring distance for the most stable conformational increases. This can be explained by the better electron donor-acceptor effect carbazole and Edot rings and the smaller steric effect caused by the oxygen atom in the Cbz-Edot and Cbz-furane, which is smaller than the sulfur atom in the Cbz-thiophene. The computed values for length distance in (Cbz-Edot) are close to the experimental values of Carbazole.[35,36]

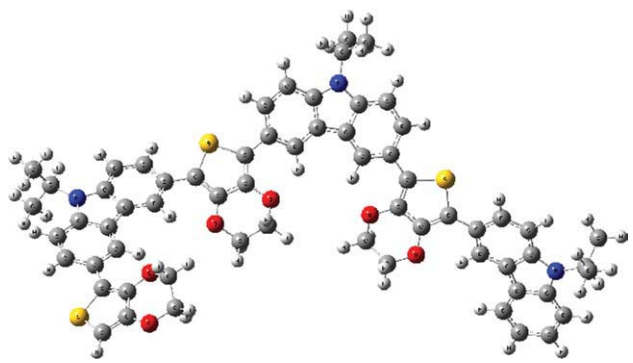

Figure 3 Optimized structure of $(Cbz\text{-}Edot)_3$ obtained by B3LYP/6-311G(d,p) level, for the neutral form. [Color figure can be viewed in the online issue, which is available at wileyonlinelibrary.com.]

TABLE III
Optimized Structural Parameters [Bond Length (in Å) and Inter-Ring Twisting Angle (°)] of Oligomers (Cbz-Edot)$_n$ (n =1–3) in Neutral, Polaronic, and Bipolaronic States Obtained by B3LYP/6-311G(d,p) Level

	Neutral			Polaronic			Bipolaronic		
No of monomers	1	2	3	1	2	3	1	2	3
C_1 C_2	1.361	1.361	1.361	1.374	1.364	1.364	1.387	1.371	1.367
C_2 C_3	1.432	1.432	1.432	1.416	1.429	1.431	1.405	1.420	1.424
C_3 C_4	1.375	1.375	1.374	1.408	1.382	1.379	1.438	1.397	1.389
C_4 C_5	1.465	1.465	1.465	1.425	1.455	1.461	1.390	1.438	1.448
C_5 C_6	1.400	1.401	1.400	1.425	1.409	1.407	1.447	1.424	1.414
C_6 C_7	1.393	1.393	1.393	1.373	1.387	1.391	1.359	1.379	1.384
C_7 C_8	1.445	1.446	1.446	1.451	1.452	1.450	1.454	1.461	1.455
C_8 C_9	1.396	1.392	1.393	1.391	1.378	1.386	1.386	1.369	1.379
C_9 C_{10}	1.388	1.400	1.401	1.394	1.417	1.414	1.404	1.432	1.420
C_{10} C_{11}	–	1.463	1.463	–	1.435	1.448	–	1.418	1.437
C_{11} C_{12}	–	1.374	1.374	–	1.400	1.390	–	1.416	1.398
C_{12} C_{13}	–	1.428	1.428	–	1.408	1.418	–	1.396	1.410
C_{13} C_{14}	–	1.374	1.374	–	1.399	1.390	–	1.416	1.396
C_{14} C_{15}	–	1.463	1.463	–	1.438	1.448	–	1.417	1.439
C_{15} C_{16}	–	1.401	1.401	–	1.415	1.414	–	1.429	1.382
C_{16} C_{17}	–	1.393	1.393	–	1.382	1.387	–	1.371	1.456
C_{17} C_{18}	–	1.445	1.446	–	1.447	1.452	–	1.450	1.381
C_{18} C_{19}	–	1.396	1.392	–	1.395	1.388	–	1.392	1.419
C_{19} C_{20}	–	1.388	1.401	–	1.389	1.414	–	1.393	
C_{20} C_{21}	–	–	1.463	–	–	1.449	–	–	1.436
C_{21} C_{22}	–	–	1.374	–	–	1.389	–	–	1.398
C_{22} C_{23}	–	–	1.428	–	–	1.419	–	–	1.408
C_{23} C_{24}	–	–	1.374	–	–	1.391	–	–	1.401
C_{24} C_{25}	–	–	1.463	–	–	1.450	–	–	1.433
C_{25} C_{26}	–	–	1.401	–	–	1.412	–	–	1.419
C_{26} C_{27}	–	–	1.393	–	–	1.388	–	–	1.379
C_{27} C_{28}	–	–	1.445	–	–	1.447	–	–	1.448
C_{28} C_{29}	–	–	1.396	–	–	1.397	–	–	1.393
C_{29} C_{30}	–	–	1.389	–	–	1.391	–	–	1.392
θ_1	25.2	23.9	26.2	3.0	18.4	22.5	1.1	9.1	15.5
θ_2	–	24.0	24.6	–	6.0	10.5	–	1.9	6.0
θ_3	–	23.5	23.4	–	8.0	13.9	–	0.9	11.0
θ_4	–	–	24.1	–	–	12.1	–	–	10.4
θ_5	–	–	22.5	–	–	8.0	–	–	2.2

The torsional angles and barriers to internal rotation depend on the balance of two interactions, as a consequent of the π-electrons conjugation between tow adjacent monomers, the molecules tend to remain planar, whereas the steric repulsion between hydrogens causes the molecules to twist. In comparison with the torsional angles obtained in the case of PEDOT[37,38] ($\theta_i = 180.0 \pm 5.0°$), where the anti conformation was predicted as the global minimum at different levels of theory, i.e., HF, B3LYP, B3PW91, and MP2 combined with different basis sets. The effect of insertion of PVK motive is clearly seen.

Frontier molecular orbital

To obtain a reasonable qualitative indication of the excitation properties, and of the ability of electron or hole transport, one examined the HOMO and LUMO orbitals for all oligomers of (Cbz-Edot)$_n$ (n = 1–3). Figure 4 shows that all frontier orbitals in the oligomers (Cbz-Edot)$_n$, spread over the π conjugated backbone. The HOMO possesses an antibonding character between the consecutive subunits; on the other hand, the LUMO of all oligomers generally shows a bonding character between the subunits. We note that the electronic density is predominant in the center rings compared to the extremities for the two orbitals HOMO and LUMO.

Doped structures

For the optimization of (Cbz-Edot)$_n$ (n = 1–3) structures in their polaronic and bipolaronic structures, we start from the optimized ground state oligomers structures. All oligomer structures obtained for singly and doubly oxidized state are syn-planar. The optimized structures obtained for (Cbz-Edot)$_3$, in its polaronic and bipolaronic states are sketched in Figure 5.

Table III presents the results of optimization of the oligomer parameters in their neutral, polaronic, and bipolaronic forms, so as to illustrate the change in

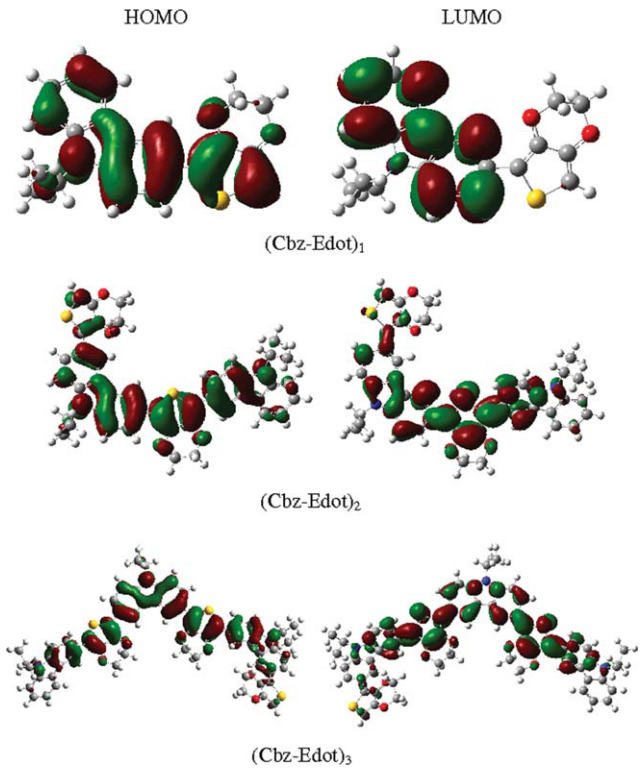

Figure 4 B3LYP/6-311G(d,p) electronic density contours of the frontiers orbitals for $(Cbz\text{-}Edot)_n$ (n = 1–3), in the neutral state. [Color figure can be viewed in the online issue, which is available at wileyonlinelibrary.com.]

oligomer structures. When we compared the bonds of the oxidized with the neutral forms, we note that the bond lengths of all the molecules changed more or less as expected: the double bonds are somewhat longer and the single ones are, however, somewhat shorter than normal C-C double and single bonds.

If it is noted that C_α are the carbons which form inter-rings bond and C_β are the other carbons, the C_α-C_β bonds increase whereas C_β-C_β decrease from neutral to polaronic state. For example, for the neutral oligomer $(Cbz\text{-}Edot)_3$, the bond C_1C_2 (1.361 Å) changes increases slightly (1.364 Å) in polaronic state and, the bond C_3C_4 increase from (1.374 Å) in neutral form to (1.379 Å) in polaronic form. The strong hydrogen-hydrogen repulsion generated by the planarity of the rings is responsible for the longer inter-ring bonds.

When the second electron is removed, the structure becomes more quinoidic (Table III), the bond lengths C_α-C_β increase while C_β-C_β ones decrease.

The effect of doping is clearly seen in the case of $(Cbz\text{-}Edot)_3$, a large reduction of dihedral angles θ_i is noticed (22.5, 10.5, 13.9, 12.1, and 8.0° compared to 26.2, 24.6, 23.4, 24.1, and 22.5° in the neutral state, respectively). The effect is more marked in the bipolaronic state (15.5, 6.0, 11.0, 10.4, and 2.2° compared with the values in the neutral state, respectively). This indicates that doping significantly enhances the planarity of the oligomer structure.

Figure 6 illustrates the variations of the bond lengths according to the bond numbers from $(Cbz\text{-}Edot)_3$, with the neutral, polaronic, and bipolaronic states.

When compared the neutral oligomers with the doped structures, the bonds become shorter, while the double ones become longer. The inter-rings bonds are longer than normal double bonds. A quinoid-like distortion emerges as a result of the oxidation of the oligomers. The region with a clearly distinct quinoid structure extends over four units, which is consistent with the *ab initio* HF and DFT calculations performed by Casado et al.[39] for substituted oligothiophenes. The optimized geometry of the dicationic copolymers $(Cbz\text{-}Edot)_n$ (n = 1–3) indicates the formation of the positive bipolaron defect localized in the middle of the molecule and extending over the adjacent repeat units. The charged species are characterized by a reversal of the single/double C—C bonds pattern; the geometry process thus induces the appearance of a strong quinoid character within the molecule.

Structural parameters of the copolymers $(Cbz\text{-}Edot)_3$ in its quinoidic form (polaronic and bipolaronic) indicate

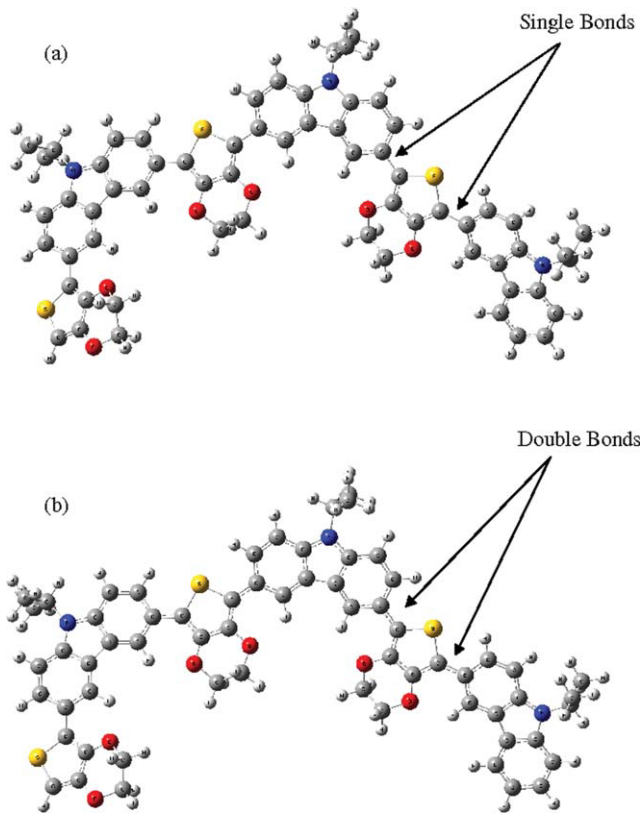

Figure 5 Optimized structures of the $(Cbz\text{-}Edot)_3$ in its polaronic (a) and bipolaronic (b) states obtained by B3LYP/6-311G(d,p) level. [Color figure can be viewed in the online issue, which is available at wileyonlinelibrary.com.]

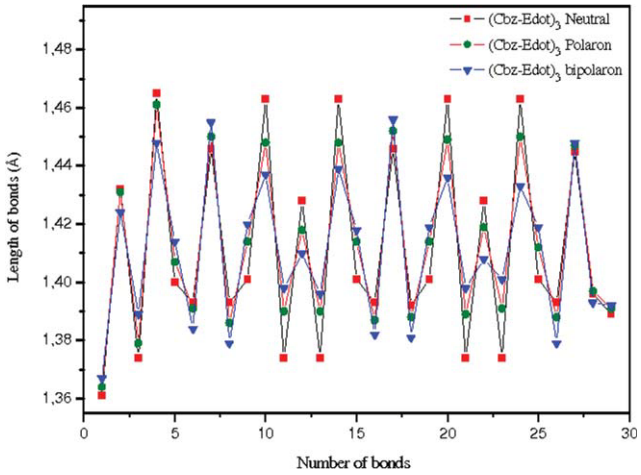

Figure 6 Comparison of the bond lengths from (Cbz-Edot)$_3$ in the neutral, polaronic and bipolaronic states. [Color figure can be viewed in the online issue, which is available at wileyonlinelibrary.com.]

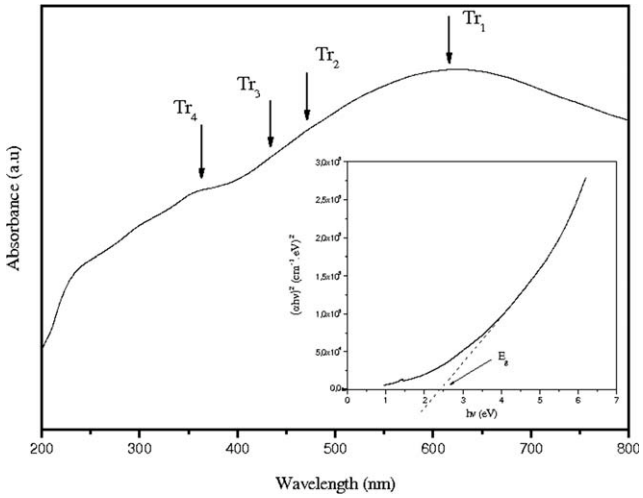

Figure 7 Optical absorption of (PVK-PEDOT) copolymer, and inset: representation of $(\alpha h\nu)^2$ versus $h\nu$ for the calculation of E_g.

that the rings at the ends preserve their aromatic character, whereas the central processing units present a quinoid character. For the oxidized (Cbz-Edot)$_3^{+\cdot}$, the innermost rings are characterized by quinoidic structure.

UV-Visible

We present in Table IV the calculated absorption λ_{max} (nm), oscillator strength (OS) and transition energies E_{tr} (eV), of the oligomers (Cbz-Edot)$_n$ (n = 1–3) in neutral form. These values are calculated by TD-DFT, CIS, and ZINDO methods, starting with optimized geometry obtained by B3LYP/6-311G(d,p) level.

The theoretical values obtained by ZINDO and TD-DFT calculations are almost similar. The analysis of the table shows that the theoretical values of λ_{max} increases with the number of monomers of several oligomers.

Figure 7 shows the experimental absorption spectra measured for (PVK-PEDOT) from powder, in the range of 200–800 nm at room temperature. The copolymer exhibits high absorbance in the studied UV-Visible range. The UV-Visible absorption spectra shows a maximum peak at 620 nm, with subpeaks or shoulders at 363.8, 435.1, and 473.2 nm, these bands can be attributed to the π–π* transition. It should be noted that, the absorption maximum (λ_{max}) values are sufficient to consider applications of these materials in the opto-electronic field.[40] As mentioned, PVK absorbs entirely in the UV region (λ_{max} < 350 nm).[41] Furthermore the absorption detected in the UV-Visible spectrum of our copolymer centered at 363.8 nm is attributed to π–π* transition, due to the presence of PVK in the copolymer (PVK-PEDOT). On the other hand, the optical absorption spectrum of the PEDOT film exhibits a broad band centered at 525 nm.[42,43] We conclude that the transition located at 620 nm in the UV-Visible spectrum of (PVK-PEDOT) is a result of a π–π* transition due to the presence of the PEDOT moieties in our copolymer.

Moreover, the energy corresponding to the π–π* transition is depending on the delocalization of the π electrons system. The absorption coefficient "α," was determined from the transmission spectra using the following relationship[44,45]:

$$\alpha(h\nu) = \frac{1}{d}\ln\left\{\frac{(1-R^2)}{2T} + \left|R^2 + \left[\frac{(1-R^2)}{2T}\right]^2\right|^{\frac{1}{2}}\right\}$$

where d is the thickness, T is the transmittance, and R is the reflectance.

The energy of the band gap, E_g, was calculated through the equation: $(\alpha h\nu)^2 = A(h\nu - E_g)$, where A is a constant and a direct gap is supposed.

TABLE IV
Calculated Absorption λ_{max} (nm), Transition Energy (eV) and Oscillator Strength (OS) for All Oligomers (Cbz-Edot)$_n$ (n = 1–3)

Method		1	2	3
ZINDO	λ_{max} (nm)	347.84	403.21	414.03
	E_{tr} (eV)	3.564	3.075	2.995
	OS	0.673	1.034	1.646
TD/B3LYP/ 6-311G(d,p)	λ_{max}(nm)	315.17	387.74	408.27
	E_{tr}(eV)	3.934	3.197	3.036
	OS	0.464	1.389	1.524
CIS/6-311G(d,p)	λ_{max} (nm)	244.95	292.90	300.85
	E_{tr} (eV)	5.061	4.233	4.120
	OS	0.740	1.314	2.258

TABLE V
The HOMO, LUMO, E_g, Pol.1, Pol.2, ΔE_P, B.pol.1, B.pol.2, and $\Delta E_{B.p}$ Values of Energy (in eV) of (Cbz-Edot)$_n$, (n =1–3) in Neutral, Polaronic, and Bipolaronic Forms

	Neutral form			Polaron			Bipolaron		
No of monomers	HOMO	LUMO	E_g	Pol_1	Pol_2	ΔE_p	$B.Pol_1$	$B.Pol_2$	ΔE_{Bp}
$n = 1$	−5.10	−0.92	4.18	−8.80	−4.90	3.90	−12.89	−11.20	1.69
$n = 2$	−4.73	−1.11	3.62	−7.35	−4.31	3.04	−9.79	−9.07	0.72
$n = 3$	−4.65	−1.15	3.50	−6.72	−3.90	2.82	−8.50	−8.13	0.37
$n = \infty$	–	–	3.13	–	–	2.25	–	–	0.27
Exp[a]	–	–	–	–	–	2.45	–	–	–

[a] In this work, optical band gap derived from the absorption spectrum of a powders polymer.

Figure 7, shows the optical absorption spectra, and the inset shows the representation of $(\alpha h\nu)^2$ versus $(h\nu)$ used for the calculation of the energy gap E_g. The band gap is obtained by extrapolating the straight portion of the curve to the zero absorption coefficient.[46]

The band gap value, determined for the copolymer (PVK-Pedot), is $E_g = 2.45$ eV.

Band gaps

Traditionally, charged states in conjugated polymers and oligomers have been discussed in terms of a one-electron band model.[47] Only one singly charged defect leads to the appearance of two new levels inside the band gap (Pol.1 and Pol.2). The lower level is occupied by one electron. Removal of a second electron results in the formation of a bipolaron which is characterized by the appearance of two new levels (B.pol.1 and B.pol.2) more distant from the band edges than the polaron levels.[48,49]

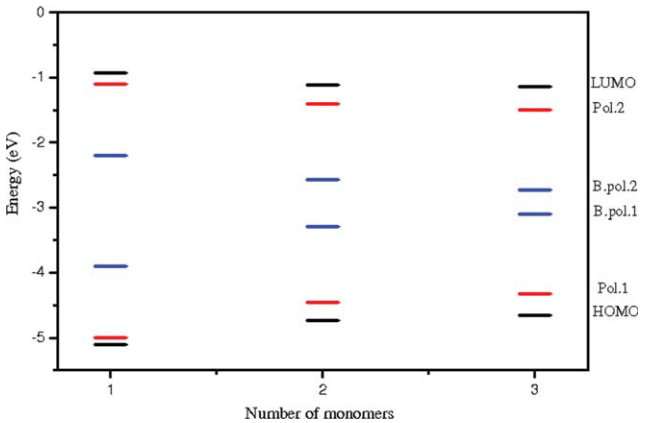

Figure 8 Schematic representation of the HOMO and LUMO levels (dark) of neutral, Pol.1, Pol.2 energy levels (red) of polaron state and B.pol.1, B.pol.2 energy levels (blue) of bipolaron state of oligomers (Cbz-Edot)$_n$, obtained by B3LYP/6-311G(d,p) level. [Color figure can be viewed in the online issue, which is available at wileyonlinelibrary.com.]

The values of the energy of the HOMO, LUMO, E_g (between HOMO and LUMO), Pol.1, Pol.2, and ΔE_P (between Pol.1 and Pol.2) and B.pol.1, B.pol.2, and $\Delta E_{B.p}$ (between B.pol.1 and B.pol.2), obtained by B3LYP/6-311G(d,p) level, are listed in Table V, and sketched in terms of relative energy in Figure 8 for neutral and doped states. The experimental gap energy value obtained from the optical absorption spectrum, of the copolymer (PVK-PEDOT), is presented also for comparison.

Figure 8 shows the variations of the gap energy as a function of the number of monomers at neutral and doping forms. For the bipolaronic state, when the number of monomers increases, a weak energy of gap is obtained (0.37 eV for $n = 3$).

As is usual in π-conjugated systems, in the neutral form, with the increasing conjugation lengths the HOMO energies increase, whereas the LUMO energies decrease in all series. On the other hand, in the polaronic and bipolaronic states, the HOMO and LUMO energies increase with the conjugation lengths (Table V).

The oligomer (Cbz-Edot)$_3$, at doped state, has the particularity of having a gap (2.82 eV) which concord well with that of the polymer determined from the absorption spectrum (2.45 eV).

Interestingly, for the copolymer studied in this work, good agreements between the (HOMO-LUMO) gap from the polaronic state, and experimental observation have been demonstrated with density functional theory (DFT). Optical band gap derived from the absorption spectrum of the polymer (PVK-PEDOT) in its powder form is 2.45 eV; this value is 5% higher than that calculated by HOMO-LUMO (2.25 eV). The major factor responsible for this difference in energy obtained by the method of calculation and that found experimentally is that solid-state effects (like polarization and intermolecular packing forces) have been neglected in the calculations.[50] If we consider that there is about 0.2 eV[51] of difference between the theoretical band gaps calculated for doped state, our theoretical results, reported in Table V, are in agreement with the experimental results.

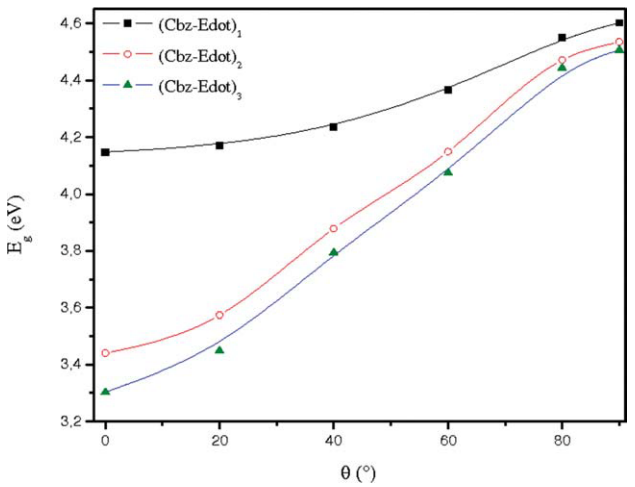

Figure 9 Evolution of the gap energy E_g (eV) of various oligomers $(Cbz\text{-}Edot)_n$ (n = 1–3) in this neutral form as a function of the torsion angle θ (°). [Color figure can be viewed in the online issue, which is available at wileyonlinelibrary.com.]

Evolution of the gap

To study the effect of the insertion of the monomers on the optoelectronic properties of the polymer in this neutral form, one represented on the Figure 9, the evolution of the energy of gap according to the angle of torsion between two adjacent units (Cbz and Edot).

The gap energy increases with the angle of torsion between two adjacent units, according to the reduction in the electronic delocalization π, the site of the curves relating to $(Cbz\text{-}Edot)_1$ and $(Cbz\text{-}Edot)_2$, below the curve from $(Cbz\text{-}Edot)_3$, indicates the increase in the delocalization of the electrons π in last oligomer, which improves the optoelectronic properties of polymer.

For a comparison, we present in Table VI the calculated HOMO, LUMO and E_g gap energy from the neutral state, of the oligomers $(Cbz\text{-}Cbz)_n$,[52] with the oligomers $(Cbz\text{-}Edot)_n$ (n = 1–3). When we compare the various values of calculated gap of the longest oligomer, we note that the energy gaps in $(Cbz\text{-}Edot)_3$ (3.50 eV) are dramatically lower than that in $(Cbz\text{-}Cbz)_3$ (4.16 eV), on the other hand, when we inspect the results obtained for $(EDOT)_n$,[37] the gap energy obtained by B3LYP/6-31G(d) level in the case $n = 3$ (E_g = 3.67 eV) is higher than that in $(Cbz\text{-}Edot)_3$, which indicates that, the additive conjugated monomers, facilitate the decreasing of the energy gaps. On the other hand, the calculated λ_{max} of $(Cbz\text{-}Cbz)_3$ (λ_{max} = 332.89 nm) is lower than that of $(Cbz\text{-}Edot)_3$ (λ_{max} = 414.03 nm). From these results we can conclude that the introduction of Edot, in the carbazole structure, influence dramatically the optoelectronic properties of the copolymers.

TABLE VI
The HOMO, LUMO, and E_g (eV) of $(Cbz\text{-}Cbz)_n$ and $(Cbz\text{-}Edot)_n$ (n =1–3), Obtained by B3LYP/6-311G(d,p) Level

Oligomers	HOMO (eV)	LUMO (eV)	E_g (eV)
$(Cbz\text{-}Cbz)_n$[a]			
$n = 1$	−5.02	−0.66	4.36
$n = 2$	−4.86	−0.66	4.20
$n = 3$	−4.82	−0.66	4.16
$n = \infty$	–	–	4.02
$(Cbz\text{-}Edot)_n$			
$n = 1$	−5.10	−0.92	4.18
$n = 2$	−4.73	−1.11	3.62
$n = 3$	−4.65	−1.15	3.50
$n = \infty$	–	–	3.13

[a] The HOMO, LUMO, and E_g of neutral form of $(Cbz\text{-}Cbz)_n$.[52]

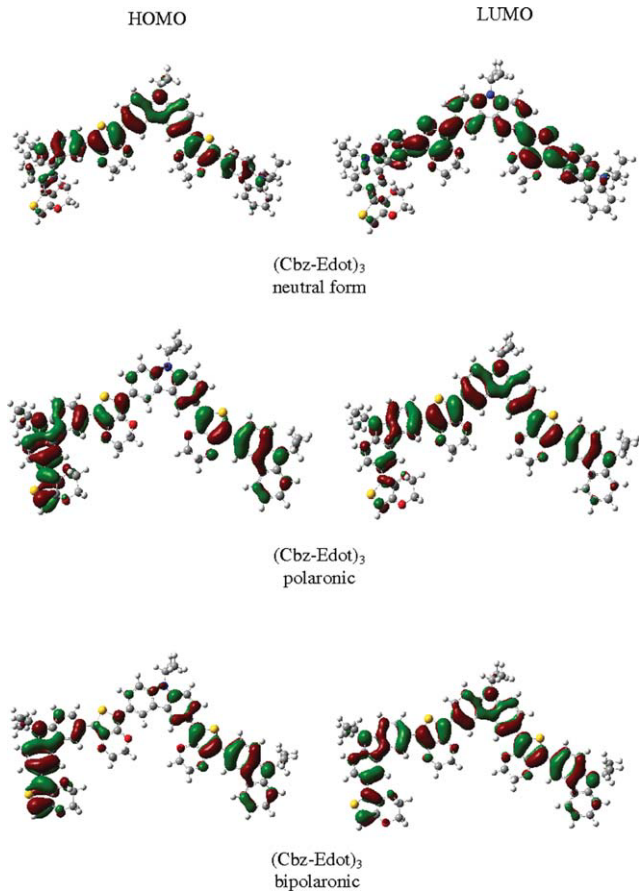

Figure 10 The HOMO and LUMO orbitals of $(Cbz\text{-}Edot)_3$ in the neutral, polaronic and bipolaronic states by B3LYP/6-311G(d,p) level. [Color figure can be viewed in the online issue, which is available at wileyonlinelibrary.com.]

Characters of the frontier orbitals of oligomer $(Cbz\text{-}Edot)_3$, in the neutral, polaronic, and bipolaronic states

It is useful to examine the HOMOs and LUMOs for $(Cbz\text{-}Edot)_3$ in the neutral, polaronic, and bipolaronic states. The relative ordering of the occupied

and virtual orbitals provides a reasonable qualitative indication of the excitation properties,[53–55] and of the ability of electron or hole transport. The electron density of HOMO and LUMO of the oligomer (Cbz-Edot)$_3$, in the neutral, polaronic and bipolaronic states are plotted in Figure 10. This figure shows that all frontier orbitals in the oligomer of all states under study spread over the whole π conjugated bakbone. In general, the HOMO has the antibonding character between the subunits; on the other hand, the LUMO of the oligomer of all states shows a bonding charcter between the subunits.

This figure illustrate also the variations of the electronic density of the two orbitals HOMO and LUMO. For the orbital HOMO in a doped state, the electronic density is predominant in the extremities compared to the center, and it is significant in the EDOT being located at the oligomer extrimity, with the bipolaronic state, for the orbital LUMO, the variation of the electronic density according to the states polaronic then bipolaronic is weak. These remarks confirm the conjugated character of the studied polymer.

CONCLUSION

In this work, theoretical and experimental results are investigated to describe polymerization of conjugated monomers based on carbazole and ethylenedioxythiophene. The torsional potentials for neutral, polaronic, and bipolaronic for all oligomers, were obtained from B3LYP/6-311G(d,p) calculations. It was deduced that the most stable conformation for the neutral form of oligomers is the syngauche conformation. In the doped states, the oligomers become more planar and show a quinoidal character.

The values of optical absorption λ_{max} in a neutral state are calculated by the three methods (ZINDO, TD-DFT, and CIS), these values increase with the number of monomers.

The gap energy calculated for the all oligomers, decreases with the chain length, this decrease is also observed when passing from the neutral to the polaronic and to the bipolaronic forms. The value of the gap energy of the polymer (PVK-PEDOT), as measured experimentally, is appreciably equal to that calculated for the oligomer (Cbz-Edot)$_3$ in this doped form; this oligomer is therefore, a useful model to understand electronic properties of the parent polymer.

References

1. Skotheim, T. A.; Elsenbaumer, R. L.; Reynolds, J. R. Handbook of Conducting Polymers, 2nd ed.; Marcel Dekker: New York, 1998.
2. Zotti, G.; Schiavon, G.; Zecchin, S.; Morin, J. F.; Leclerc, M. Macromolecules 2002, 35, 2122.
3. Garnier, F.; Horowitz, G.; Peng, X.; Fichou, D. Adv Mater 1990, 2, 562.
4. Gill, R. E.; Malliaras, G. G.; Wildeman, J.; Hadziioannou, G. Adv Mater 1994, 6, 132.
5. Grazulevicius, J. V.; Strohriegl, P.; Pielichowski, J.; Pielichowski, K. Prog Polym Sci 2003, 28, 1297.
6. Yang, L.; Kang Feng, J.; Min Ren, A.; Zhong Sun, J. Polymer 2006, 47, 1397.
7. Burroughes, J. H.; Bardley, D. D. C.; Brown, A. R.; Marks, R. N.; Mackay, K.; Friend, R. H.; Burns, P. L.; Holms, A. B. Nature 1990, 347, 539.
8. Ben Khalifa, M.; Vaufrey, D.; Bouazizi, A.; Tardy, J.; Maaref, H. Mater Sci Eng C 2002, 21, 277.
9. Groenendaal, L.; Jonas, F.; Freitag, D.; Pielartzik, H.; Reynolds, R. Adv Mater 2000, 12, 481.
10. Apperloo, J.; Groenendaal, L. B.; Verheyen, H.; Jayakannan, M.; Janssen, R. A.; Dkhissi, A.; Beljonne, D.; Lazzaroni, R.; Brédas, J. L. Chem Eur J 2002, 8, 2384.
11. Yu, J.; Holdcroft, S. Chem Mater 2002, 14, 3705.
12. Pei, Q.; Zuccarello, G.; Ahlskog, M.; Inganäs, O. Polymer 1994, 35, 1347.
13. Sakmeche, N.; Aaron, J. J.; Fall, M.; Aeiyach, S.; Jouni, M.; Lacroix, J. C.; Lacaze, P. C. Chem Commun 1996, 24, 2723.
14. Dkhissi, A.; Beljonne, D.; Lazzaroni, R.; Louwet, F.; Groenendaal, L.; Brédas, J. L. Int J Quantum Chem 2002, 91, 517.
15. Dkhissi, A.; Louwet, F.; Groenendaal, L.; Beljonne, D.; Lazzaroni, R.; Brédas, J. L. Chem Phys Lett 2002, 359, 466.
16. El Malki, Z.; Hasnaoui, K.; Bejjit, L.; Haddad, M.; Hamidi, M.; Bouachrine, M. J Non-Crystalline Solids 2010, 356, 467.
17. El Malki, Z.; Hasnaoui, K.; Bouzzine, S. M.; Bejjit, L.; Haddad, M.; Hamidi, M.; Bouachrine, M. SRX Chem Volume 2010, 1–8 (2010). Article ID 346843, doi: 10.3814/2010/346843.
18. Mitschke, U.; Bauerle, P. J Mater Chem 2000, 10, 1471.
19. Leclerc, M. J Polym Sci Polym Chem 2001, 39, 2867.
20. Kraft, A.; Grimsdale, A. C.; Holmes, A. B. Angew Chem Int Ed 1998, 37, 402.
21. Dimitrakopoulos, C. D.; Malenfant, P. R. L. Adv Mater 2002, 14, 99.
22. Katz, H. E.; Bao, Z. J Phys Chem B 2000, 104, 671.
23. Becke, A. D. J Chem Phys 1993, 98, 5648.
24. McLean, A. D.; Chandler, G. S. J Chem Phys 1980, 72, 5639.
25. Wachters, A. J. H. J Chem Phys 1970, 52, 1033.
26. Hay, P. J. J Chem Phys 1977, 66, 4377.
27. McGrath, M. P.; Radom, L. J Chem Phys 1991, 94, 511.
28. Foresman, J. B.; Head-Gordon, M.; Pople, J. A.; Frisch, M. J. J Chem Phys 1992, 96, 135.
29. Stanton, J. F.; Gauss, J.; Ishikawa, N.; Head-Gordon, M. J Chem Phys 1995, 103, 4160.
30. Yang, S. Y.; Kan, Y. H.; Yang, G. C.; Su, Z. M.; Zhao, L. Chem Phys Lett 2006, 429, 108.
31. Ma, J.; Li, S.-H.; Jiang, Y.-S. Macromolecules 2002, 35, 1109.
32. Zhang, G.-L.; Ma, J.; Jiang, Y.-S. Macromolecules 2003, 36, 2130.
33. Frisch, M. J.; Trucks, G. W.; Schlegel, H. B.; Scuseria, G. E.; Robb, M. A.; Cheeseman, J. R.; Montgomery, J. A.; Vreven, T.; Kudin, K. N., Jr.; Burant, J. C.; Millam, J. M.; Iyengar, S. S.; Tomasi, J.; Barone, V.; Mennucci, B.; Cossi, M.; Scalmani, G.; Rega, N.; Petersson, G. A.; Nakatsuji, H.; Hada, M.; Ehara, M.; Toyota, K.; Fukuda, R.; Hasegawa, J.; Ishida, M.; Nakajima, T.; Honda, Y.; Kitao, O.; Nakai, H.; Klene, M.; Li, X.; Knox, J. E.; Hratchian, H. P.; Cross, J. B.; Adamo, C.; Jaramillo, J.; Gomperts, R.; Stratmann, R. E.; Yazyev, O.; Austin, A. J.; Cammi, R.; Pomelli, C.; Ochterski, J. W.; Ayala, P. Y.; Morokuma, K.; Voth, G. A.; Salvador, P.; Dannenberg, J. J.; Zakrzewski, V. G.; Dapprich, S.; Daniels, A. D.; Strain, M. C.; Farkas, O.; Malick, D. K.; Rabuck, A. D.; Raghavachari, K.; Foresman, J. B.; Ortiz, J. V.; Cui, Q.; Baboul, A. G.; Clifford, S.; Cioslowski, J.; Stefanov, B. B.; Liu, G.; Liashenko, A.; Piskorz, P.; Komaromi, I.;

Martin, R. L.; Fox, D. J.; Keith, T.; Al-Laham, M. A.; Peng, C. Y.; Nanayakkara, A.; Challacombe, M.; Gill, P. M. W.; Johnson, B.; Chen, W.; Wong, M. W.; Gonzalez, C.; Pople, J. A. GAUSSIAN 03, Revision B. 04; Gaussian: Pittsburgh, PA, 2003.
34. Belletête, M.; Bédard, M.; Leclerc, M.; Durocher, G. J Mol Struct (Theochem) 2004, 679, 9.
35. Basak, B. S.; Lahiri, B. N.; Indian. J. Pure Appl Phys 1969, 7, 234.
36. Pan, J.-H.; Chiu, H.-L.; Wang, B.-C. J Mol Struct (Theochem) 2005, 725, 89.
37. Alemán, C.; Armelin, E.; Iribarren, J. I.; Liesa, F. Synth Met 2005, 149, 151.
38. Alemán, C.; Casanovas, J. J Phys Chem 2004, 108, 1440.
39. Casado, J.; Hernàndez, V.; Ramirez, F. J.; López Navarrete, J. T. J Mol Struct (Theochem) 1999, 463, 211.
40. Bouachrine, M.; Lère-Porte, J. P.; Moreau, J. J. E.; Serein-Spirau, F.; Augusta Silva, R.; Lmimouni, K.; Dufour, C. Phys Chem News 2002, 6, 73.
41. Xia Wu, H.; Qiong Qiu, X.; Fang Cai, R.; Xiong Qian, S. Appl Surf Sci 2007, 253, 5122.
42. Zanardi, C.; Terzi, F.; Pigani, L.; Heras, A.; Colina, A.; Lopez-Palacios, J.; Seeber, R. Electrochim Acta 2008, 53, 3916.
43. Beouch, L.; Tran Van, F.; Stephan, O.; Claude Vial, J.; Chevrot, C. Synth Met 2001, 122, 351.
44. Sahal, M.; Hartiti, B.; Mari, B.; Ridah, A.; Mollar, M. Afrique Sci 2006, 02, 245.
45. Hernández-Fenollosa, M. A.; López, M. C.; Donderis, V.; González, M.; Marí, B.; Ramos-Barrado, J. R. Thin Solid Films 2008, 516, 1622.
46. Sahal, M.; Marí, B.; Mollar, M. Thin Solid Films 2009, 517, 2202.
47. Brédas, J. L.; Themans, B.; André, J. M. Phys Rev 1982, B26, 6000.
48. Bouzzine, S. M.; Bouzakraoui, S.; Bouachrine, M.; Hamidi, M. J Mol Struct (Theochem) 2005, 726, 271.
49. Bouzzine, S. M.; Bouzakraoui, S.; Hamidi, M.; Bouachrine, M. Asian J Chem 2007, 19, 1651.
50. Yang, Li.; Feng, J.-K.; Liao, Y.; Ren, A.-M. Optical Mater 2007, 29, 642.
51. Salzner, U.; Lagowski, J. B.; Pickup, P. G.; Poirier, R. A. Synth Met 1998, 96, 177.
52. Hasnaoui, K.; Makayssi, A.; Hamidi, M.; Bouachrine, M. J Iran Chem Res 2008, 1, 67.
53. Gong, Z.; Lagowski, J. B. J Mol Struct (Theochem) 2008, 866, 27.
54. Suramitr, S.; Hannongbua, S.; Wolschann, P. J Mol Struct (Theochem) 2007, 807, 109.
55. Yang, L.; Feng, J.-K.; Ren, A.-M. Polymer 2005, 46, 10970.